APPLICATION OF A COPPER VAPOUR LASER TO INVESTIGATION OF SHOCK AND BLADE INTERACTION IN A SHOCK TUBE

R J PARKER & J B BROWNELL

Advanced Research Laboratory
Rolls-Royce plc
PO Box 31, Derby

1.0 Introduction

The shock tube is a well known and much used device for aerodynamic research. In the study described herein a shock tube has been used to simulate the behaviour of an aero-engine compressor stator vane during surge. Stator vanes were tested both singly and in a cascade to observe their dynamic behaviour under loading from a backward travelling shock-wave.

Conventional instrumentation was augmented by two optical techniques. Shadowgraph flow visualization allowed the shock front transition through the cascade to be visualized, while optical grid projection allowed the dynamic reaction of the vane to be measured. For both optical techniques a novel light source was employed. A copper vapour laser was used, providing an intense train of short optical pulses capable of freezing these fast-moving phenomena.

In this paper the experimental optical equipment is described and the results of the optical measurements are presented and briefly discussed. A more complete discussion of the shock tube study and the use made of these techniques to verify computer models of the vane behaviour have also been published[1].

2.0 The Shock Tube Experiment

Surge is a complicated phenomenon, the physics of which have been described by Mazzawy[2]. In the process a stall spreads around the entire annulus of the compressor. This blocks the flow and a shock wave, propagating forward in the engine, is formed. This shockwave imposes a severe loading on many mechanical components in the opposite sense to the loading they are designed to sustain.

It is not possible in a shock tube facility such as this to simulate exactly the conditions in an aeroengine undergoing surge. It was felt, however, that data could be gathered from a shock tube experiment that could be compared with computer models of the aerodynamics and mechanics of the same experiment. If reasonable agreement was observed, the computer model could then, with confidence, be extended to model the behaviour of the blades under typical engine surge conditions. This philosophy is summarised schematically in Figure 1.

The shock tube is a much-used experimental tool in research[3]. The Advanced Research Laboratory shock tube facility is shown schematically in Figure 2. A driver section is separated from the driven section by an aluminium diaphragm. The driver and driven section are filled with gases to a predetermined pressure. The pressure in the driver section is then increased until the aluminium diaphragm bursts, launching a shock wave into the driven section. This process is very repeatable. The shock wave passes through the working section where the blades are situated. At the other end of the working section, the travelling shock wave passes through a thin melamine diaphragm and into an evacuated dump tank. This greatly reduces the reflection of the shock wave back into the working section.

Figure 2. shows the two blade configurations which were tested. The first was a single blade in a rectangular section duct. This configuration allowed full field measurement of the dynamic deflection of the aerofoil surface using the projected grid method. A large glass window formed one wall of the duct. The conventional instrumentation for this configuration consisted of two miniature piezo-electric pressure transducers (one on each side of the blade, in the duct wall, over the tip) and strain gauges (three) on the aerofoil surface. The second configuration of the working section was as a cascade of three full blade passages. In this configuration the shock front traverse of the cascade could be visualized by shadowgraph, and the deflection of the tips of the blades could again be measured using the grid projection method. Optical access was via a circular Perspex window mounted over the blade tips. Conventional instrumentation consisted of an array of eight pressure transducers measuring the central passage of the cascade. These were mounted in a circular plug which replaced the optical window. It was thus not possible to take pressure and optical measurements on the same tube run. Additional fixed instrumentation consisted of two Kistler pressure probes up-stream of the blade which were used to measure the pressure difference and velocity of the travelling shock wave.

Typical test conditions were as follows:-

Driven section - Nitrogen - 690kPa
Driver section - Helium - 4000kPa
Shock velocity at working section - 550m/s (Mach 1.6)
Pressure step across shock - 1300kPa

3.0 Optical Instrumentation

A shadowgraph technique was used to visualize the shock wave and other aerodynamic features in the cascade flow. Deflection of the blades was measured dynamically using a structured lighting technique. For both of these methods a copper vapour laser was employed as the light source, and images were recorded using a drum camera.

3.1 The Copper Vapour Laser

The copper vapour laser[4] has many properties which make it useful as an illumination source for research into high speed flow and mechanical

phenomena. The laser light emerges as a train of short (20ns) pulses with a repetition rate selectable between 2kHz and 20kHz. The light is emitted simultaneously at two wavelengths 510nm (green) and 578nm (yellow). The low divergence of the light beam provides a very small effective source size, compared for example to arc or spark light sources. This is of particular importance for shadowgraph work. The laser gives high average power (10W) and peak powers of 100kW. At optimum repetition rates the pulses each contain 2mJ of light energy. Compared to many laser sources the coherence length of the light is short (150-300mm), but since none of the techniques employed here was interferometric, this was not a problem. An additional facility afforded by the small effective source size, is the ability to couple the laser light efficiently into a fibre-optic cable. This greatly facilitates the optical arrangement and allows the laser to be positioned several metres from the test section, with just a small fibre-optic delivery system close to the working section. This also helps to reduce the possibility of electrical interference form the laser being picked-up by other instrumentation.

The particular laser used for this study was a model CU10, produced by Oxford Lasers. Compared to other copper vapour lasers, this model has the advantage of a larger range of repetition rates. It also requires only single phase, 240V, 13A supply and is air cooled; making it relatively portable. The laser head is shown schematically in Figure 3. Figure 4 shows a photograph of the laser mounted on a trolley. The power supply can be seen (centre left) below the laser head. On the right of the picture is the optics bay (cover removed) with the fibre-optic cable emerging.

The laser is a Class IV laser and thus stringent safety precautions must be enforced to prevent accidental exposure of personnel to the laser beams. The main hazard from such a laser is to the eyes from direct exposure to the beam, or exposure to light reflected from a specular object.

3.2 The Drum Camera

Recording of images for both flow visualization and deformation analysis was performed using a drum camera constructed in Rolls-Royce. The drum camera is, as its name suggests, based upon a cylindrical drum with the film wrapped around its inside. The drum is supported by a spindle and, driven by an integral air turbine, spins at up to 500rev/sec. The images formed by a lens on the axis of the drum are reflected by a stationary plane mirror at 45° onto the moving film. A solenoid operated shutter behind the lens prevents inadvertent exposure of the film before and after the required event. A side port in the camera body allows the camera to be focused, the light level to be monitored and the drum speed to be measured by a photo-electric tachometer.

The drum camera was designed originally for streak photography. It would not be suitable for photography with continuous light sources, as there is no internal shutter mechanism to form the frames. However, when used with the pulsed laser, each laser pulse forms its own sharp image. No blurring was evident in the images even with the drum having a tangential velocity

of 160m/s. The drum movement during a single 20ns laser pulse was approximately 3μm. The pulse repetition rate, drum speed and image size must all be correctly chosen to get the maximum number of images onto the film without overlap. The duration of recording is limited by the period of one revolution of the drum, this is typically 2ms. The number of images that can be recorded during one revolution of the drum is 20 to 40 frames. The laser pulse train must be of exactly the right length to ensure that images are only recorded over one revolution of the drum. The film used was Ilford FP4 monochrome, 120 format.

3.3 Timing and Time-gating

As stated earlier the laser pulse train required to be gated to the required time window (one revolution of the drum camera). To allow time for the cameras solenoid operated shutter to be opened and closed without the film becoming fogged, the laser pulsing was suppressed just before and just after the required pulse train. The sequence of events leading to the release of the pulse train can be seen in the timing diagram (Figure 5). It shows the laser output, together with the pressure impulse from the travelling shock front, which was used as the triggering signal to initiate the control sequence. The control box for this sequence of events was built in house, and allows complete control of the pulse repetition frequency, the length of the pulse train, the trigger signal level and the delay between the trigger signal and the first pulse in the train.

The result of shutting down the lasers internal triggering and then restarting triggering from the external source is that the population of copper vapour atoms in the tube increases, especially those with electrons in the ground state. Upon restarting the laser the first few pulses have a higher pulse energy than the normal output. Another effect is the suppression of the first pulse after restarting. This is a result of the plasma dynamics; a stable plasma discharge has not been not established by the time of this first pulse. The maximum time period between arming the trigger box (which stops the laser pulsing) and then firing the laser is of the order of 60 seconds. A delay greater than this causes the laser to cool down too much, resulting in low output power.

3.4 Shadowgraph Flow Visualization

The shadowgraph technique has been used extensively in the visualization of shocks in wind tunnels and other experiments since its discovery in 1880 by Dvorak[6]. In most experimental arrangements the illumination is collimated and passes through the test section. It is deviated by the shock front, or other flow feature, to produce a caustic and shadow on a screen on the far side of the flow section. The shadowgraph technique is sensitive to the second derivative of density in the field of view perpendicular to the light rays.

In the shock tube arrangement the conditions are different, as there is no direct line of sight through the working section. The experimental arrangement is shown in Figure 6. The shock tube working section with

blades fitted through the rear wall has a perspex window giving optical access to the cascade section. The illumination is delivered from the Cu10 laser by the fibre optic delivery system and formed into a nominally collimated beam by a single element lens. The laser triggering is initiated by the step input from the upstream pressure transducer as the shock front passes it. A variable delay can be introduced to prevent the laser from triggering too early, or to shift the position at which the shock front is visualized in the cascade. Adjustment of the delay time between test shots allowed the repeatable shock fronts and their interaction with the cascade to be visualized with a temporal resolution greater than that provided by the pulse sequence for a single event.

3.5 Grid Projection

In order to quantify the displacement of the blade during and after the shock front's impact, a grid projection technique was used. The basic principle is that the projected grid remains stationary in space while the blade moves within the grid. Analysis of photographs allows the blade motion to be determined. The measurement resolution is determined by the pulse repetition frequency of the laser and the pitch of the projected grid pattern in the direction perpendicular to the projection axis. For the single blade tests full-field measurements of the aero-foil surface were possible, while in the cascade the grids were projected onto the blade tips, and tip movement measured.

The optical arrangement for transient deformation analysis on the single blade is shown in Figure 7. The single blade is mounted in the shock tube through the top and optical access provided by glass windows on the sides. A grating is imaged onto the blade surface at an angle of 45° to the shock tube axis. By projecting the fringes at such an angle the blade movement along the line of sight can be observed as fringe movements across the blade surface. One disadvantage of this arrangement is that the fringe volume has only a limited depth of focus, but the expected displacements of the blade were sufficiently small for this not to be a problem. The grating is placed in the projector at an angle of 22.5° to the normal so that the plane of best focus for the fringe volume lies parallel to the shock tube axis. Illumination for the fringe projector is provided by the copper vapour laser via the fibre optic delivery system and collimating optics.

The arrangement for tip photography of the cascade blade displacements is very similar to that for transient deformation analysis of the single blade. The fringe volume was in this case projected onto the blade tips perpendicular to the shock tube axis. The leading and trailing edge tip movements were determined by reference to the coarse fringes in the finer fringe pattern, the movement being assumed to be perpendicular to the fringe direction.

4.0 Results

The results of shadowgraph flow visualization are shown in Figure 8 (flow is from right to left). It shows the first eight frames from a typical film. Time zero is arbitrarily chosen as the time when the shock arrives at the up-stream edge of the blades. It can be seen from this that only one frame contains the main shock within the cascade. The repetition rate of the laser is too slow to show detail of the shock transit on a single tube run.

By altering the delay it was possible to step the shock through the passage on successive runs of the shock tube. Figure 9 shows an edited sequence of photographs showing the shock traversing the passage. Features of particular note are the relative delay in the shock front across the blade. It is this which exerts a moment on the blade. Also of interest are reflections of the shock from the blade and the vortex formed as the shock leaves the passage.

Figure 10 shows the computer prediction[1] of the shock traverse at similar time intervals. It is not possible for the computer to model the shock as an infinite gradient in pressure, thus the contours are more spread out. The leading contour may, however, be taken as a good indication of the shock position. Good agreement is observed with the measured results.

The results of grid projection on the single blade are shown in Figure 11. The vertical fringes have coarse reference fringes every 27th fringe and the spacing on the blade surface is approximately 0.2mm. The markings at the base of the frame act as static reference marks to assist in analysis of the images. The mechanism of fringe movement caused by blade displacement can be seen. The upper frame is at time, t=0 when the shock front has just arrived at the blade. The lower frame is at t=300μs and the blade has reached the peak of its displacement. The movement of the trailing edge (lefthand edge) tip is 1.8mm and for leading edge tip is 0.9mm.

Figure 12 shows a frame from one of the cascade transient deformation analysis tests.

Analysis of the transient deformation analysis images was conducted in several ways: (i) manual counting of fringe order at trailing and leading edges, (ii) automatic computational fringe analysis of the fringe order positions along a line adjacent to and parallel with the blade tip, or (iii) by direct comparison of images with a filtered moire technique.

A set of results for a single blade test is shown in Figure 13. The response of the blade to the shock pressure differential across it is shown. The transient deformation analysis of the blade is for three positions along the blade tip.

5.0 Conclusion

The combination of a grid projection technique and a copper vapour laser has proved successful in permitting detailed analysis of the deformation of compressor vanes after shock loading. The laser was also successfully used as a light source for shadowgraph flow visualization. For flow-visualization, the framing rate provided by the laser was too slow to allow multiple frames to be recorded during a single transit of the blade passage. However, because of the temporal stability and repeatability, it was possible to select a suitable sequence of shots from different tunnel runs showing the shock position and shape at different points in time.

The copper vapour laser is a new laser source providing a valuable and versatile new weapon in the arsenal of the experimental aerodynamicist.

6.0 Acknowledgement

The authors wish to thank Rolls-Royce plc for permission to publish this work.

7.0 References

1. NT Birch, JB Brownell, AM Cargill, MR Lawson, RJ Parker, KG Tillen, "Structural Loads due to surge in an axial compressor", Proceedings 4th International Conference on Vibration in Rotating Machines, Edinburgh, September 1988.

2. RS Mazzawy, "Surge induced loads in gas turbines", Trans. ASME J. of Engineering for Power, 102, pp162-68, 1980.

3. AG Gaydon, IR Hurle, "The shock tube in high-temperature chemical physics", Chapman Hall, London, 1963.

4. I Smilanski et al. Optics Communications, 30, pp 70, 1979.

5. W Merzkirch, "Flow Visualization", Academic Press, 1974.

6. AJ Durelli, VJ Parks, "Moiré Analysis of Strain", Prentice Hall, 1970.

PURPOSE OF SHOCK TUBE EXPERIMENTS

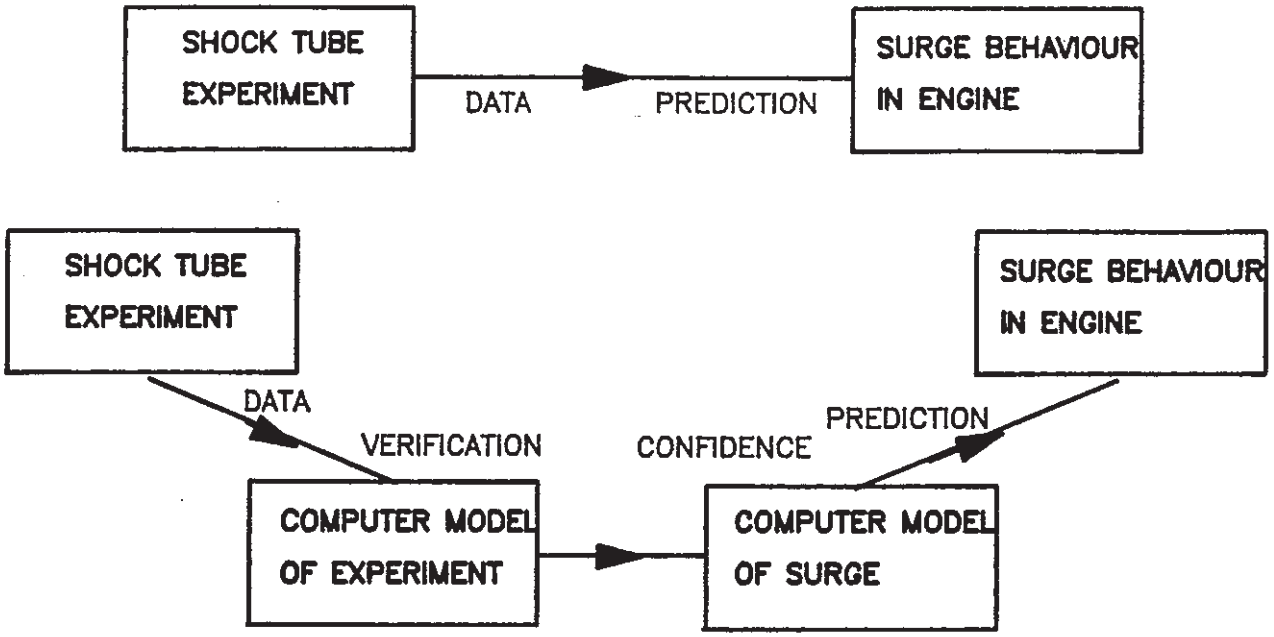

Figure 1. It is not possible to make a realistic experimental model of surge (top), but a shock tube experiment may be used to validate computer models which can then be used to predict surge (bottom)

ARL SHOCK-TUBE

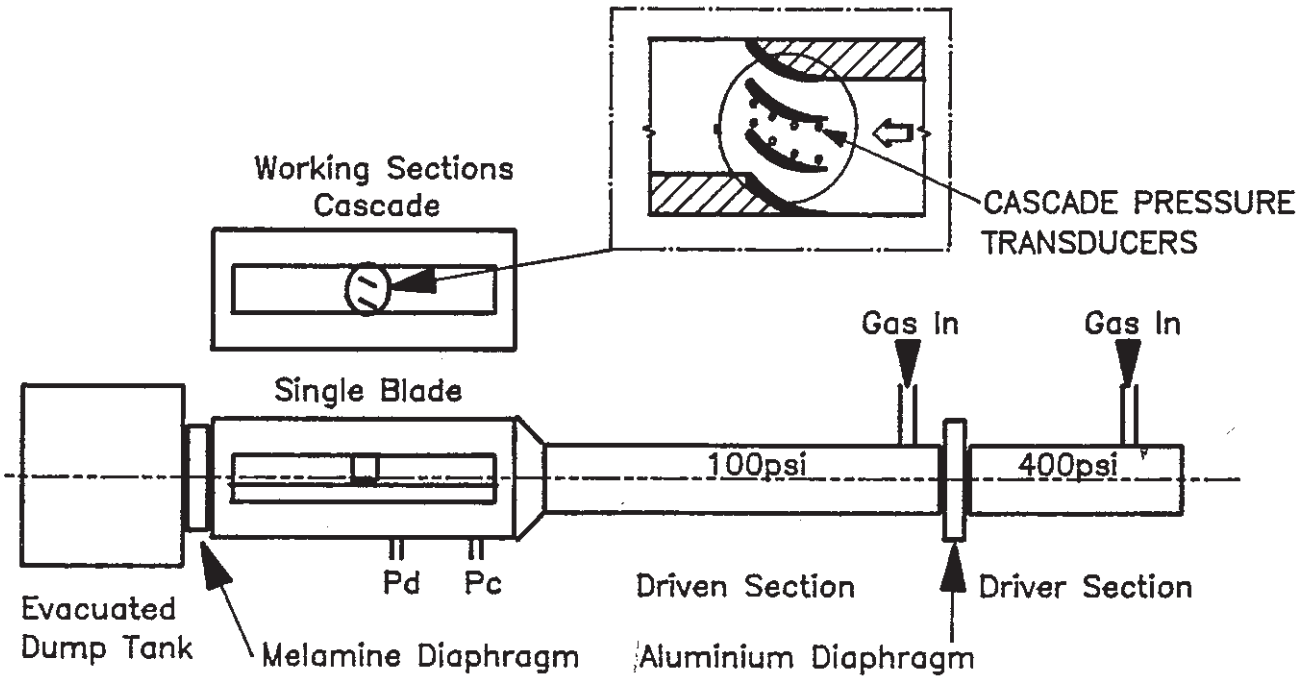

Figure 2. Schematic of the ARL shock tube showing the two blade configurations tested.

OXFP1

OXFORD LASERS CU10 COPPER VAPOUR LASER

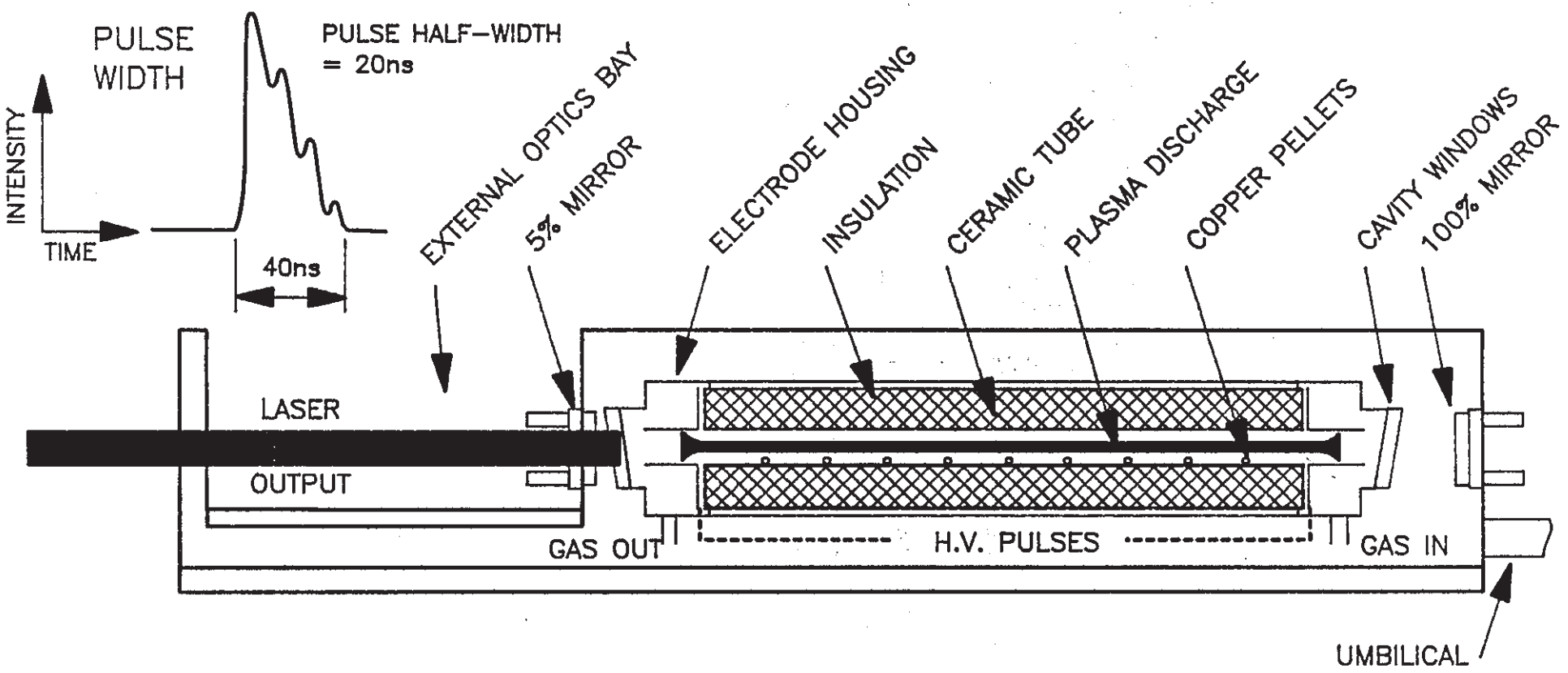

Figure 3. Schematic diagram of the copper vapour laser

OXFP2

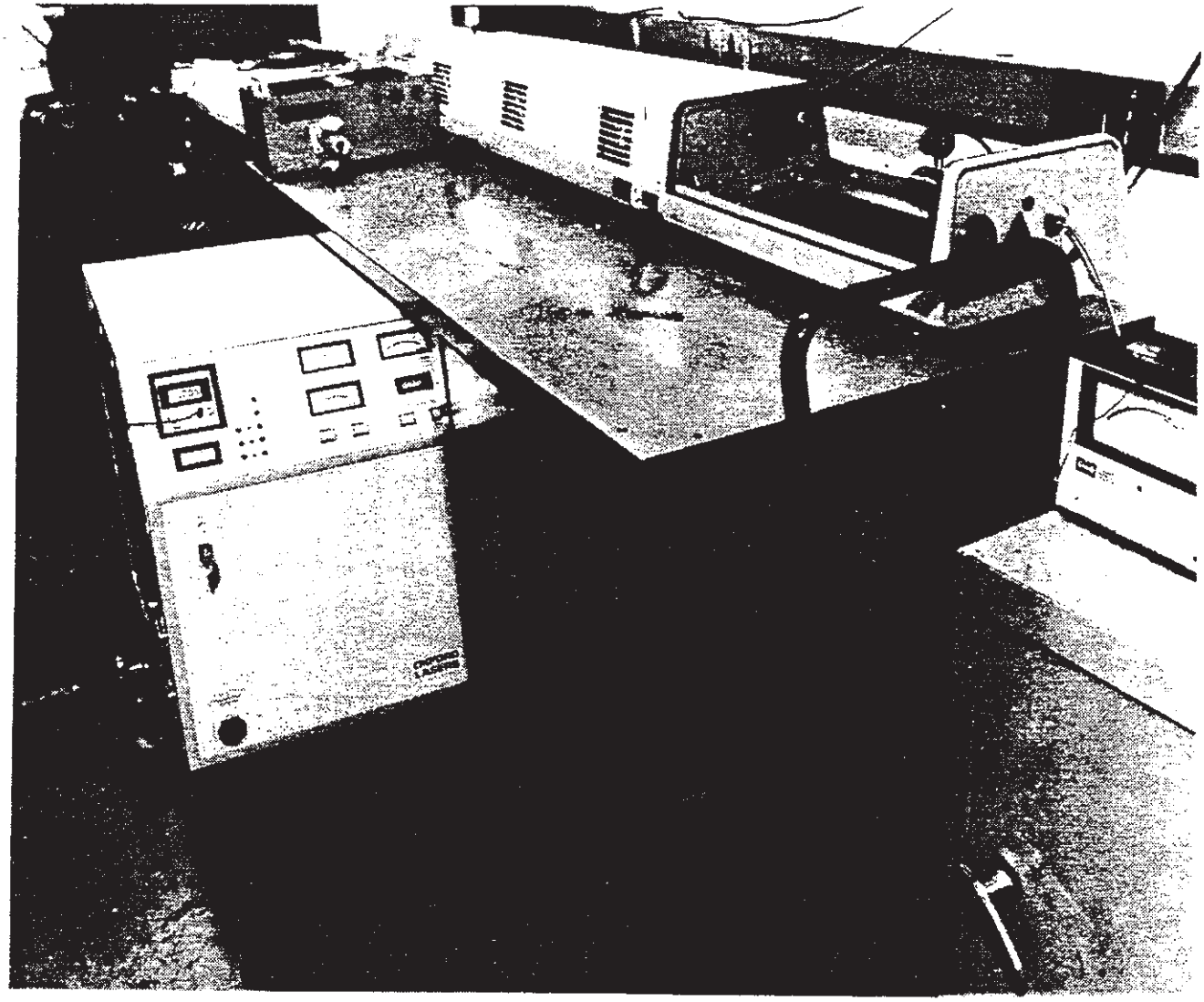

Figure 4. Photograph of the copper vapour laser

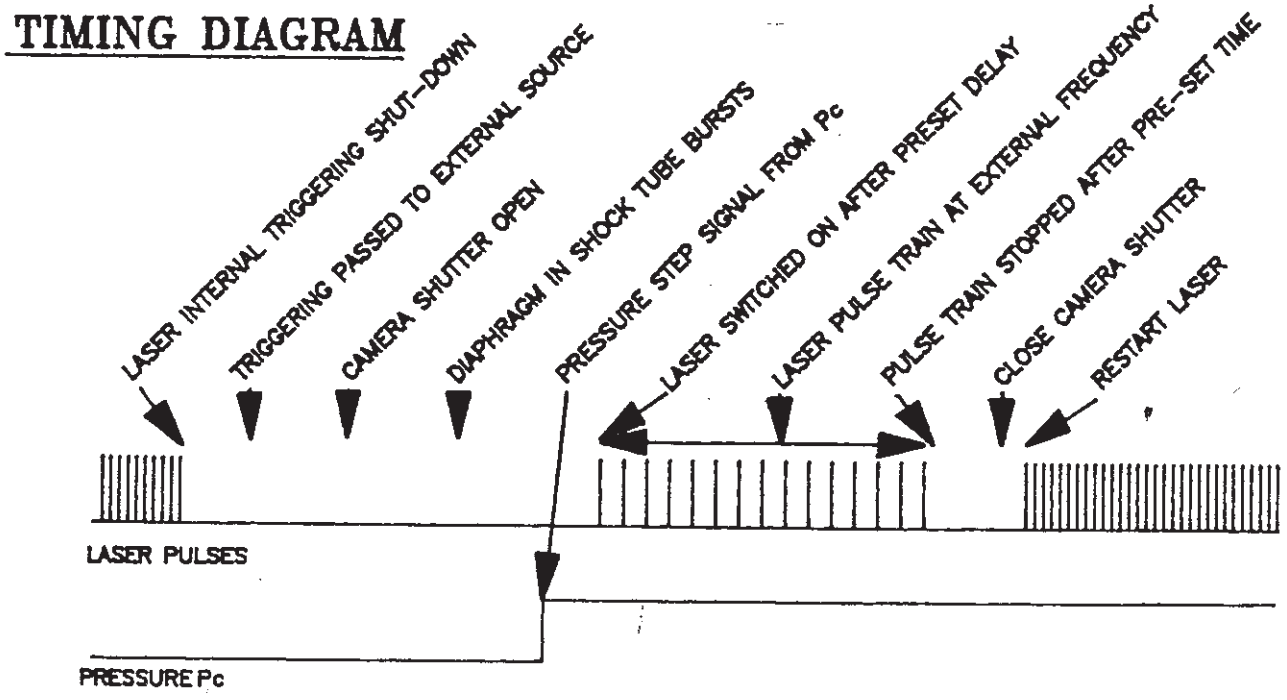

Figure 5. Laser timing diagram.

OXFP3.

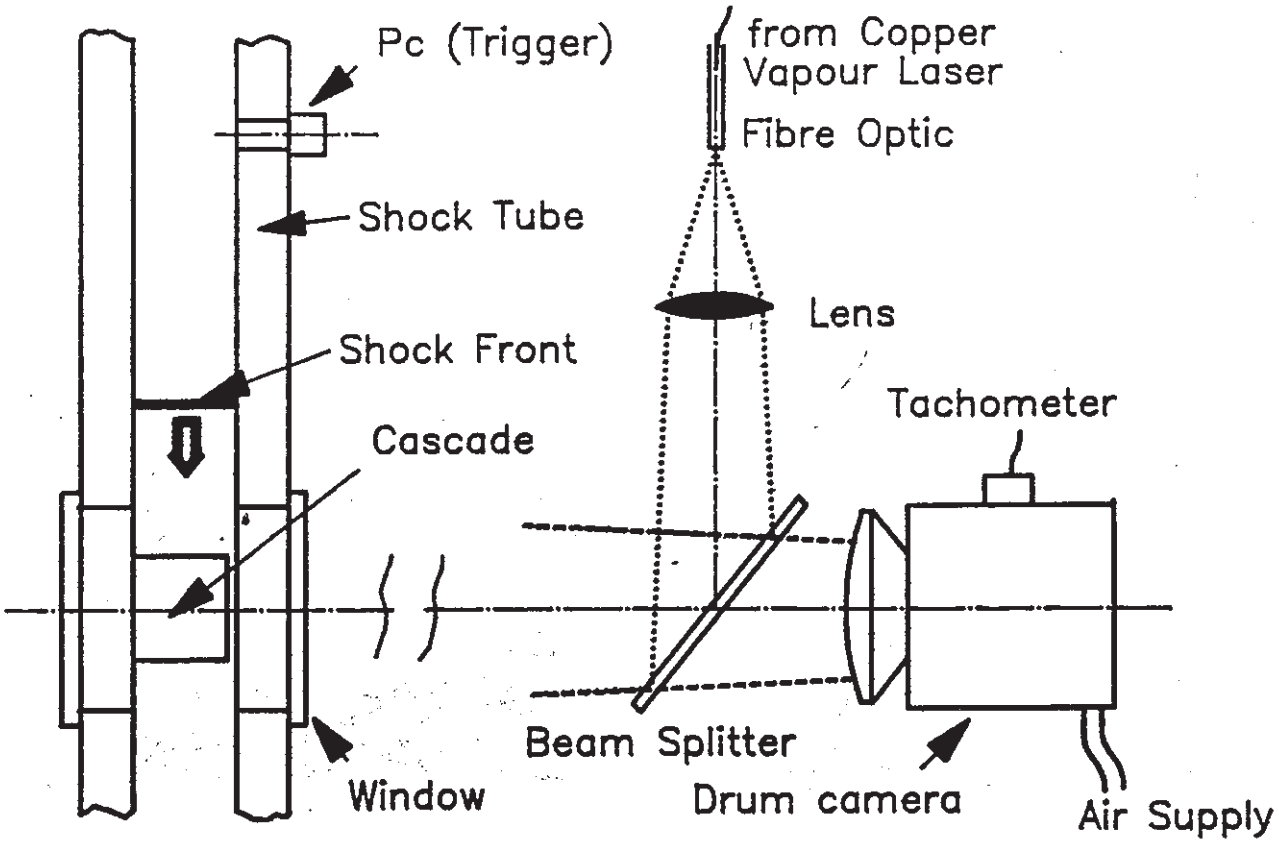

Figure 6. Apparatus for shadowgraph flow visualization

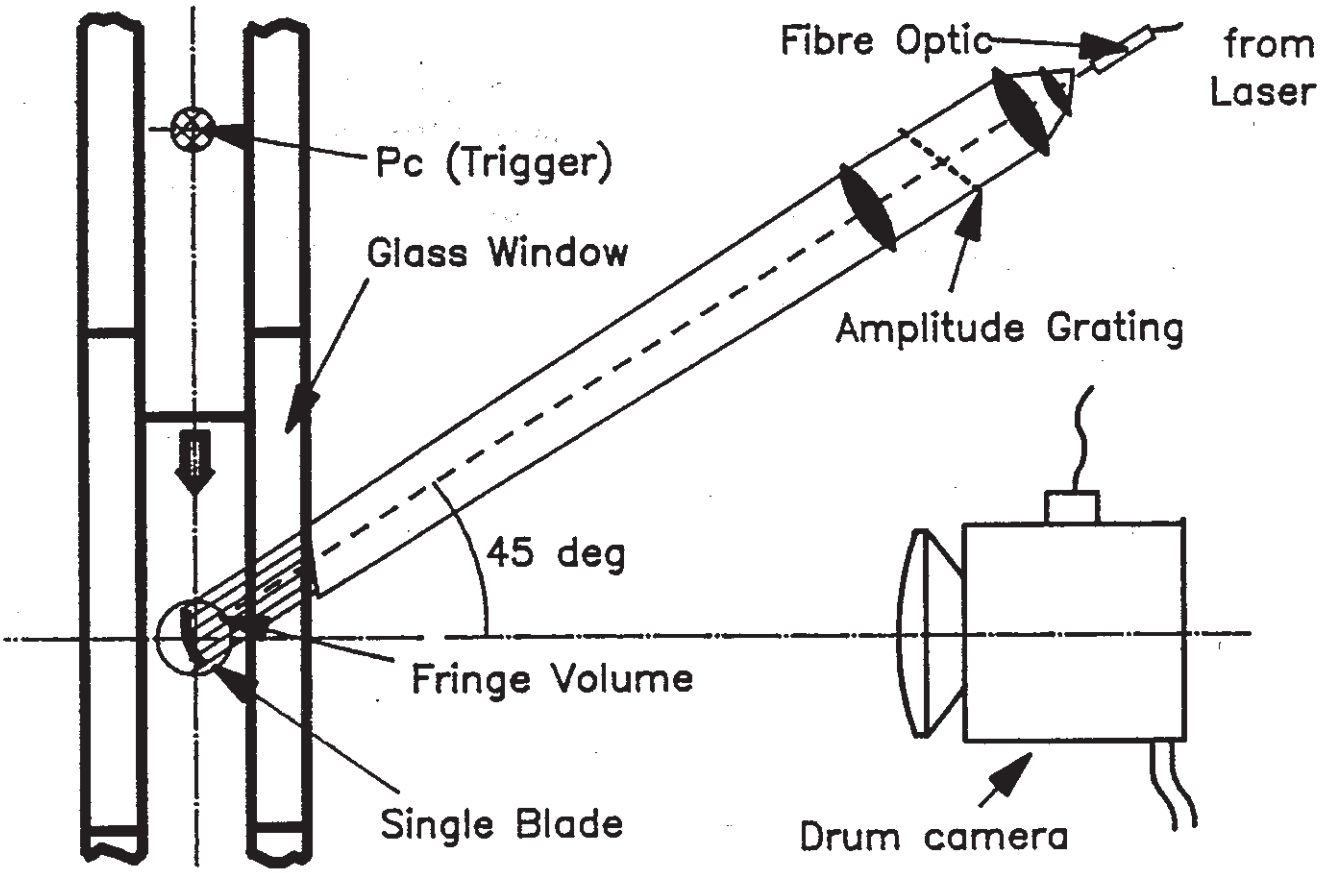

Figure 7. Apparatus for deflection measurement by grid projection

OXFP4

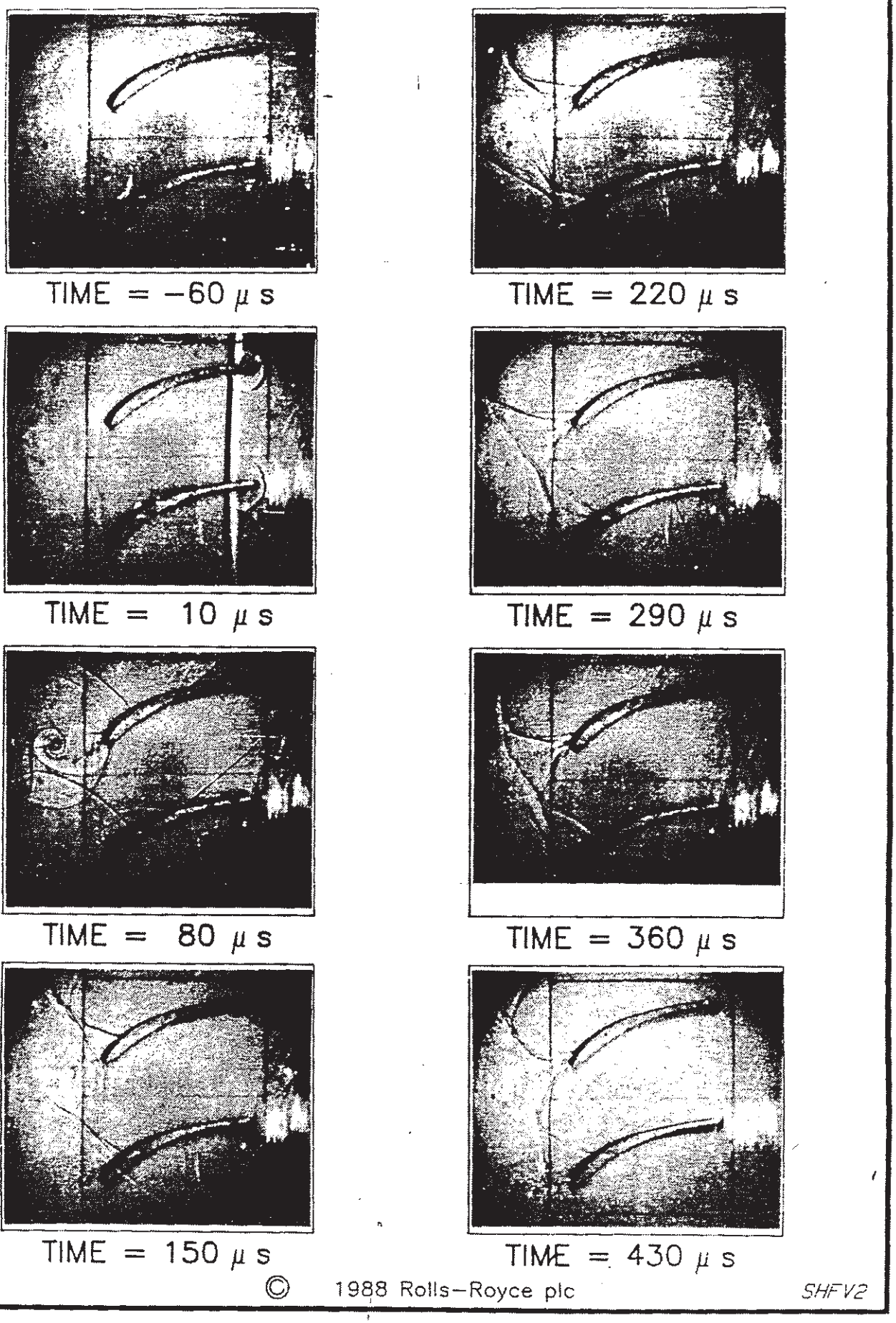

Figure 8. Sequence of shadowgraph photographs from a single shock−tube firing. Images spaced by seventy microseconds.

OXFP5

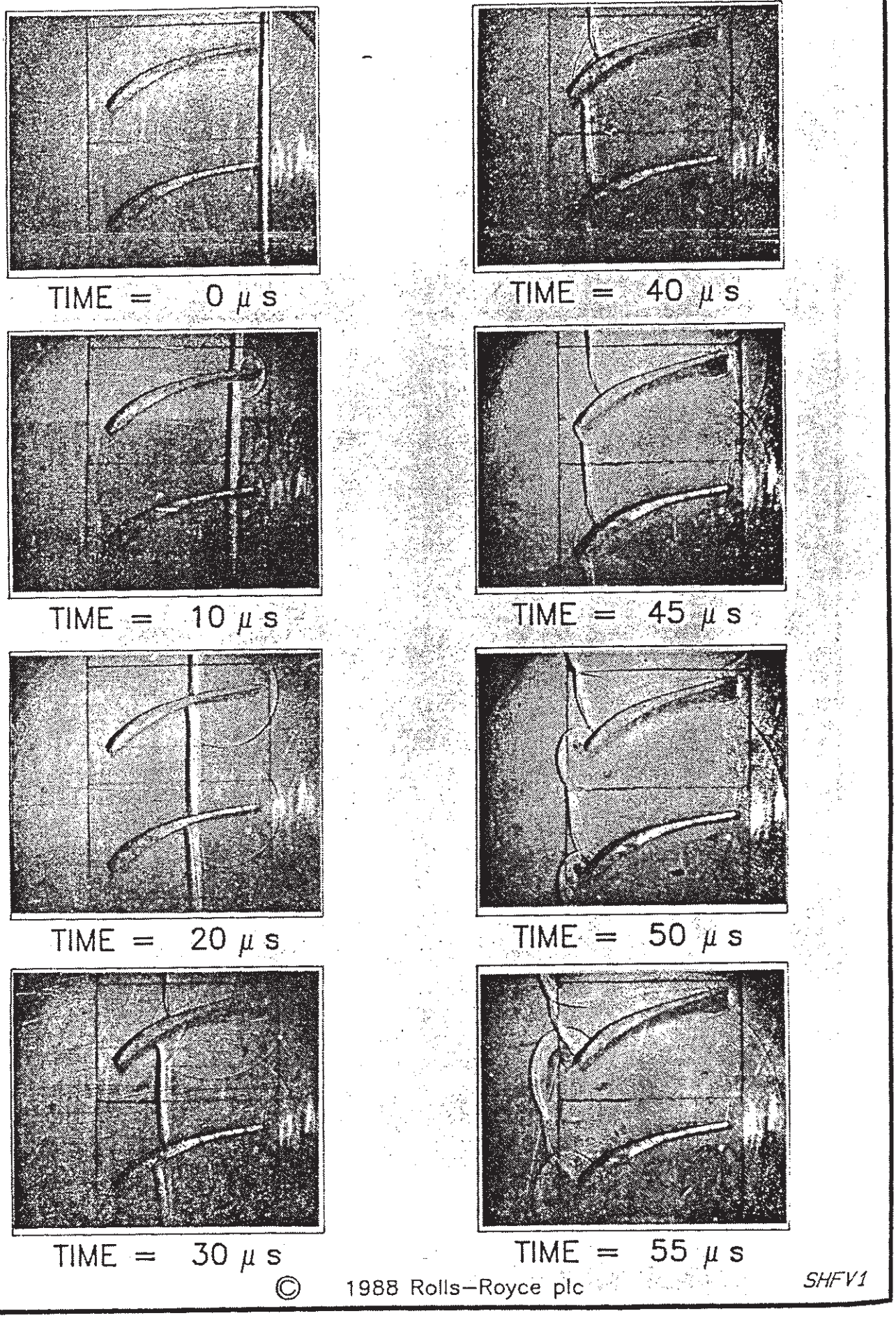

Figure 9. Edited sequence of shadowgraphs showing movement of shock wave through the cascade passage.

OXFP6

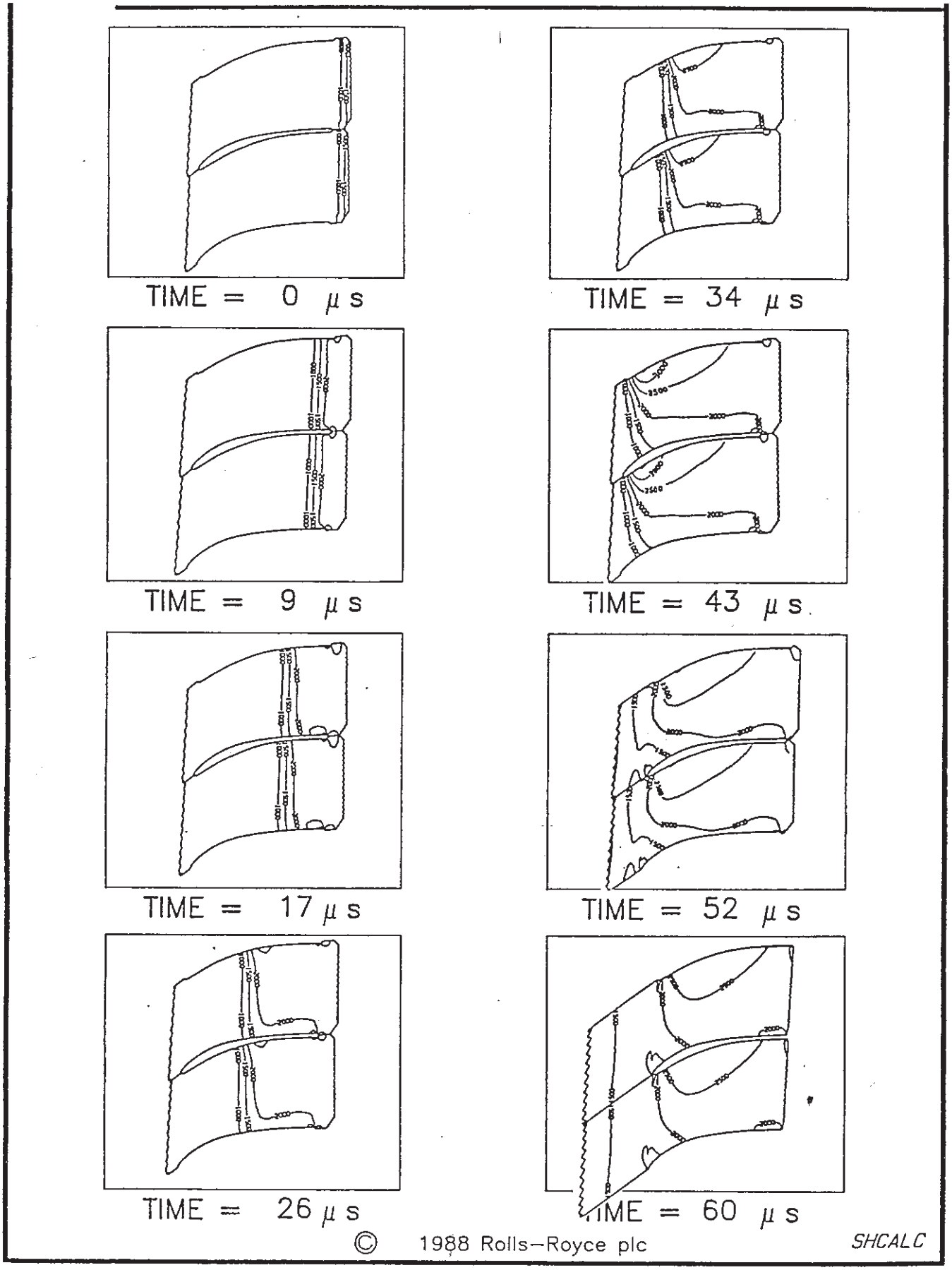

Figure 10. Computer prediction (Reference 1) of the shock wave movement through the cascade passage (cf Figure 9)

OXFP7

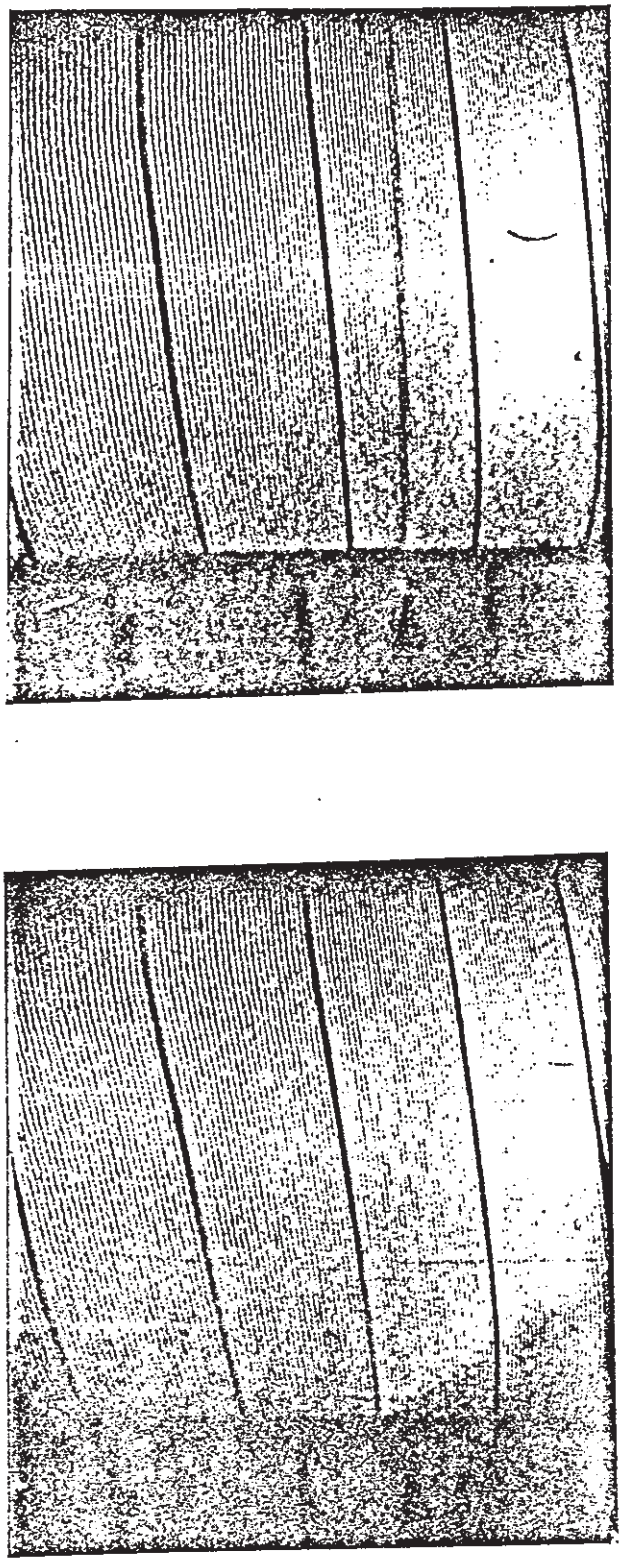

Figure 11. Examples of grid projection photographs taken 300 microseconds apart. In the upper figure the shock wave can be seen to the right of the blade centreline. Deformation of the blade (lower) can be seen from the deflection of the dark reference fringes.

OXFP8

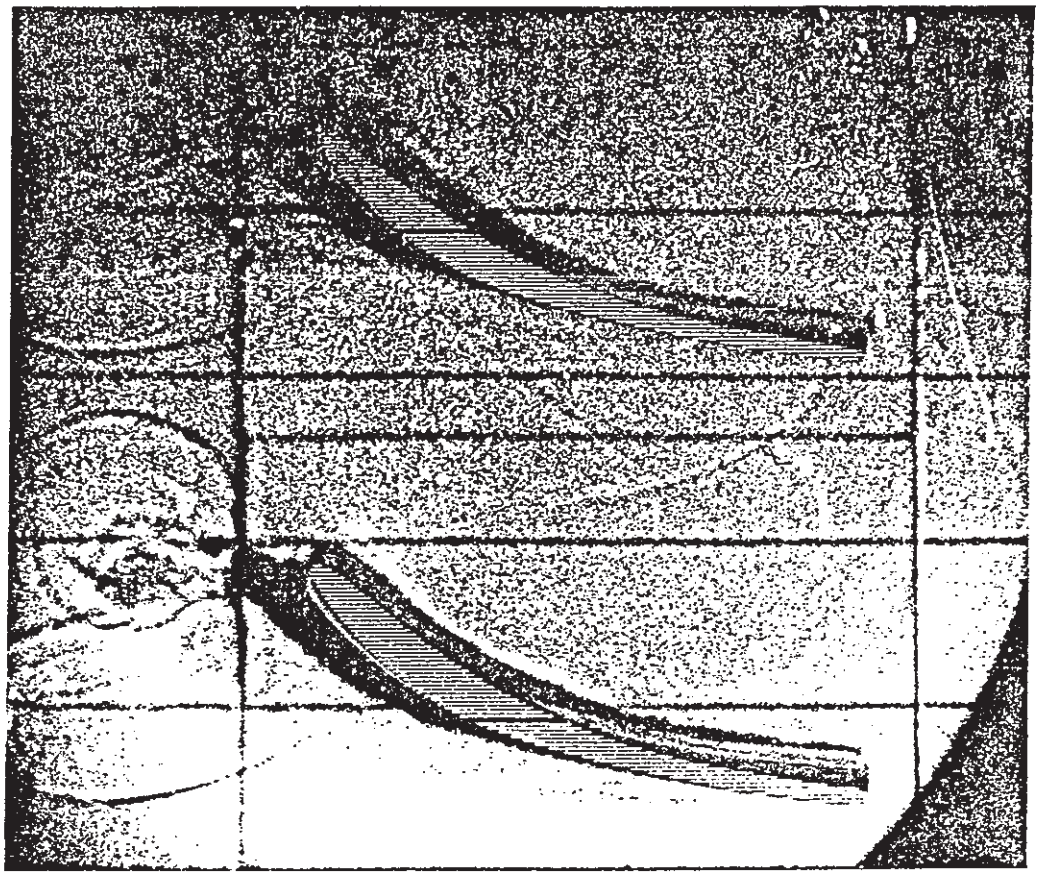

Figure 12. Example of grid projection photograph for tip displacement measurement in the cascade.

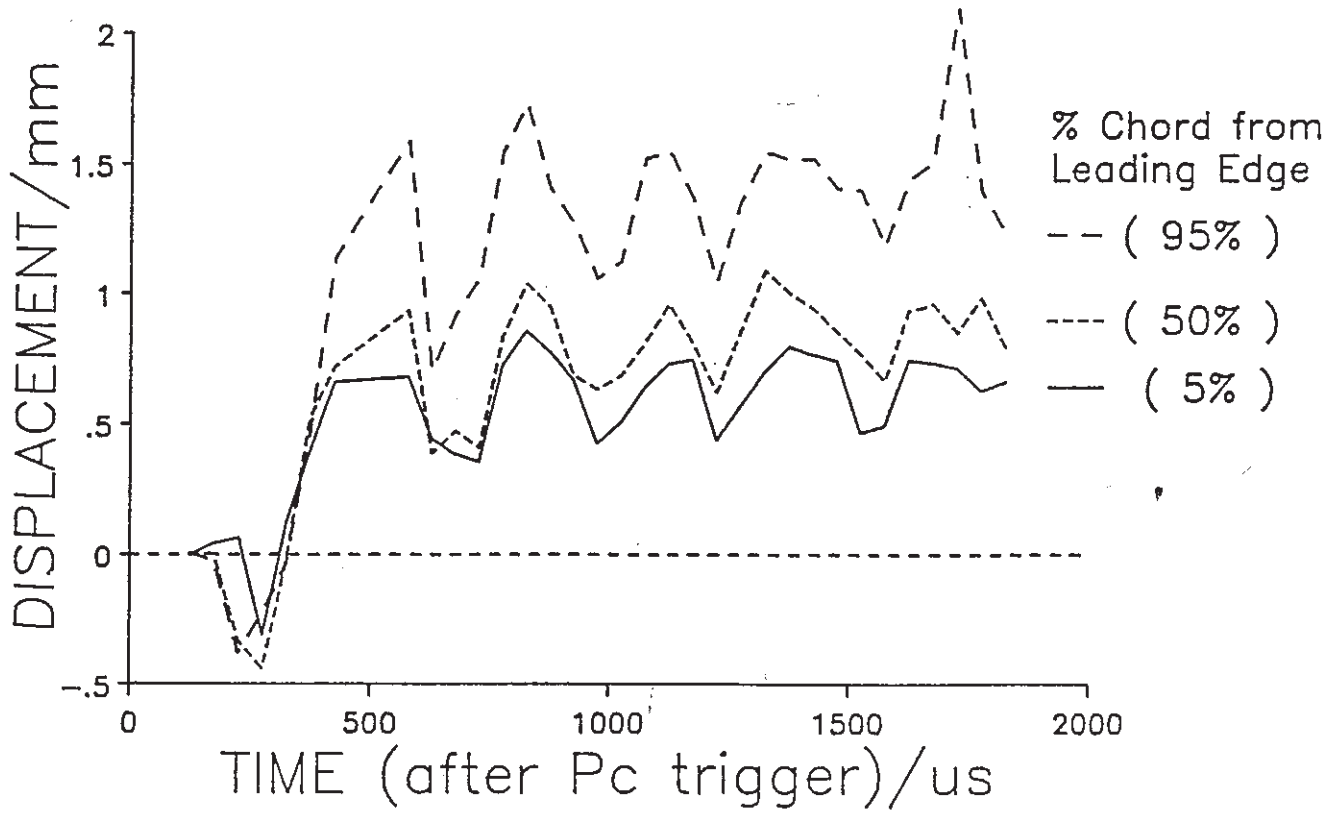

Figure 13. Example of displacement data extracted from single blade grid—projection photographs.